Single-crystal Spectral and Magnetic Studies of Dichlorotetrakis(thiourea)-iron(II) and -manganese(II)

By **M. Gerloch,*** **J. Lewis,** and **W. R. Smail,** University Chemical Laboratory, Lensfield Road, Cambridge CB2 1EW

Single-crystal and powder magnetic susceptibilities of dichlorotetrakis(thiourea)-iron(II) and -manganese(II) are reported for the temperature range 4—300 K. Polarized crystal spectra of the iron compound have been recorded at room, liquid N_2, and liquid He temperatures. The results are interpreted within the point-charge crystal-field formalism on the assumption of D_{4h} symmetry and estimates have been made of the values of *Dq*, *Dt*, and *Ds* and also of the effective spin–orbit coupling coefficient. Ambiguity concerning the signs of the distortion parameters is inherent in the iron(II) system and the results indicate $0{\cdot}6 < k = \zeta/\zeta_0 < 0{\cdot}7$, $|Dt| < 85$ cm^{-1}, and *Ds ca.* 1·8 times the magnitude of *Dt* and of the same (undetermined) sign. Within a ^6S–^4G–^4P basis for the d^5 manganese(II) system, *Ds* is irrelevant, and a simple relation between the signs of magnetic anisotropy and *Dt* emerges: here $Dt > 0$ cm^{-1}. Finally, results from these two compounds are compared with those from the nickel(II) and cobalt(II) analogues.

EXPLICIT recognition of the simultaneous effects of spin–orbit coupling, low-symmetry perturbations, and orbital reduction effects only relatively recently led to the first generally successful interpretation[1-4] of the magnetic moments of *d*-block compounds as the modified Hund formula had done for lanthanide complexes over 40 years ago.[5] The success extended to a quantitative reproduction of experimental susceptibilities in the 300—80 K temperature range by a model which was broadly transferable from one system to another. The values found for parameters by fitting theory to experiment, however, were often difficult to correlate with available structural information or with chemical intuition, occasionally being quite unreasonable; frequently they were also ambiguous. There have since been many attempts to clarify this situation,[6] experimentally, by recourse to spectral and magnetic studies of single crystals rather than to the averaged information derived from powders, and theoretically, by employing larger basis sets of wavefunctions in the calculations. Concurrent with these studies have been fresh appraisals of the significance of the various parameters used in the models: first, of orbital reduction factors[7] and presently, of the crystal-field radial integrals used to parameterize departures from cubic symmetry.[8] In studying magnetic moments and spectra of complexes of transition metals and lanthanides we are thus trying to establish a model which is of general utility, transferable from metal to metal, symmetry to symmetry, and ligand to ligand in a way that the parameter values obtained from fitting processes make sense. Primarily we are interested in the parameter values themselves, but in any given case it is just as important to assess the validity of the model and so build up confidence in its general utility.

---

[1] B. N. Figgis, *Trans. Faraday Soc.*, 1961, **57**, 198, 204.

[2] B. N. Figgis, J. Lewis, F. E. Mabbs, and G. A. Webb, *J. Chem. Soc.* (*A*), 1967, 442.

[3] B. N. Figgis, J. Lewis, F. E. Mabbs, and G. A. Webb, *J. Chem. Soc.* (*A*), 1966, 1411.

[4] B. N. Figgis, M. Gerloch, J. Lewis, F. E. Mabbs, and G. A. Webb, *J. Chem. Soc.* (*A*), 1968, 2028.

[5] J. H. Van Vleck and A. Frank, *Phys. Rev.*, 1929, **34**, 1494, 1625.

[6] M. Gerloch and J. Lewis, *Rev. Chim. min.*, 1969, **6**, 19.

[7] M. Gerloch and J. R. Miller, *Progr. Inorg. Chem.*, 1968, **10**, 1.

[8] M. Gerloch and R. C. Slade, in preparation.

We discuss here the spectral and magnetic properties of single crystals of dichlorotetrakis(thiourea)-iron(II) and -manganese(II), $M(tu)_4Cl_2$, which may be compared with similar studies of the analogous nickel(II)[9] and cobalt(II)[10] complexes. The present compounds are isomorphous[11] with $Co(tu)_4Cl_2$, being centrosymmetric with local D_{4h} symmetry, crystallizing in a tetragonal space-group in which all molecules are aligned parallel. Most work has been done on the iron(II) molecule. The manganese(II) system presents a zero-field-splitting problem of the d^5 configuration and has been studied in an essentially qualitative fashion.

EXPERIMENTAL

Powder susceptibilities of $Fe(tu)_4Cl_2$ have been measured in the temperature range 300—80 K by the Gouy method and in the range 120—4 K by an inductance method using a P.A.R. model 150 Vibrating Sample Magnetometer.

TABLE 1

Interpolated crystal and powder magnetic data for $Fe(tu)_4Cl_2$ in the temperature range 300—80 K

T/K	$10^6\bar{\chi}_M'$/c.g.s.u.	$10^6\Delta\chi_M'$/c.g.s.u.	$10^6\chi_\parallel$/c.g.s.u.	$10^6\chi_\perp$/c.g.s.u.	$\bar{\mu}$/B.M.	$\mu_\parallel$/B.M.	$\mu_\perp$/B.M.
300	11,580	200	11,710	11,510	5·27	5·30	5·25
290	11,920	230	12,070	11,840	5·27	5·29	5·24
280	12,400	260	12,570	12,310	5·27	5·31	5·25
270	12,820	290	13,010	12,720	5·26	5·30	5·24
260	13,380	320	13,590	13,270	5·27	5·31	5·25
250	13,880	360	14,120	13,760	5·27	5·31	5·24
240	14,420	400	14,690	14,290	5·26	5·31	5·24
230	15,060	460	15,370	14,910	5·26	5·32	5·24
220	15,750	520	16,100	15,580	5·26	5·32	5·24
210	16,450	590	16,840	16,250	5·25	5·32	5·23
200	17,350	660	17,790	17,130	5·27	5·33	5·24
190	18,250	760	18,760	18,000	5·27	5·34	5·23
180	19,250	860	19,820	18,960	5·26	5·34	5·23
170	20,250	990	20,910	19,920	5·25	5·33	5·20
160	21,000	1150	22,170	21,020	5·23	5·33	5·19
150	22,850	1340	23,740	22,400	5·24	5·34	5·18
140	24,600	1590	25,660	24,070	5·25	5·36	5·19
130	26,600	1900	27,870	25,970	5·26	5·39	5·20
120	29,100	2320	30,650	28,330	5·29	5·42	5·22
110	32,000	2920	33,950	31,030	5·30	5·46	5·22
100	35,300	3700	37,770	34,070	5·31	5·50	5·22
90	39,400	4600	42,470	37,870	5·32	5·52	5·22
80	45,200	5720	49,010	43,290	5·37	5·60	5·26
		$\chi_\parallel > \chi_\perp$					

TABLE 2

Interpolated powder susceptibilities and moments for $Fe(tu)_4Cl_2$ in the temperature range 120—4 K

T/K	$10^6\bar{\chi}_M'$/c.g.s.u.	$\bar{\mu}$/B.M.
120	28,820	5·26
110	31,450	5·26
100	34,600	5·26
90	38,310	5·26
80	43,100	5·25
70	49,020	5·23
60	57,140	5·24
50	68,030	5·22
40	84,750	5·21
30	112,400	5·20
20	163,900	5·12
10	312,500	5·00
5	588,200	4·85

Measurements below 80 K were calibrated by comparison with those above 80 K. Magnetic anisotropies of the tetragonal crystals, $\Delta\chi = \chi_\parallel - \chi_\perp$, have been measured in the temperature range 300—80 K by the Krishnan ' critical torque ' technique. Interpolated principal and average susceptibilities and moments are given in Table 1 for the temperature range 300—80 K and for average susceptibilities and moments from 120 to 4 K in Table 2. All results have been corrected for the diamagnetism and anisotropy of $Cd(tu)_4Cl_2$. An approximate value of 1·53 for the ratio $\chi_\parallel : \chi_\perp$ was also measured at *ca* 5 K, giving the approximate values, $\mu_\parallel =$ *ca.* 5·53, $\mu_\perp =$ *ca.* 4·47, and $\Delta\mu =$ *ca.* 1·06 B.M.

Powder susceptibilities and anisotropies of $Mn(tu)_4Cl_2$ were measured in the temperature range 300—80 K. The results, corrected for the bulk diamagnetism and magnetic anisotropy of $Cd(tu)_4Cl_2$, are in Table 3.

Crystal transmission spectra of $Fe(tu)_4Cl_2$, unpolarized at room temperature, polarized at liquid-nitrogen and liquid-helium temperatures, have been recorded with a Cary 14 spectrometer and a Cary cold-finger cryostat. The polarized spectra were recorded with light incident on a face normal to the (001) face and are shown in Figure 1.

DISCUSSION

Dichlorotetrakis(thiourea)iron(II).—Calculations for magnetic moments have used the complete ^5D free-ion term as basis; those for spectra have included ^3H and ^3D terms. The crystal-field potential of D_{4h} symmetry is parameterized by Dq, Dt, and Ds, defined as usual (see Appendix), and calculations have all involved the complete diagonalization of the appropriate basis under the simultaneous perturbation of spin–orbit coupling and D_{4h} crysyal-field. The process of fitting the experimental results for $Fe(tu)_4Cl_2$ involves simultaneous consideration of the spectrum, absolute moment

---

[9] M. Gerloch, J. Lewis, and W. R. Smail, *J. Chem. Soc.* (*A*), 1971, 2434.

[10] M. Gerloch, P. N. Quested, and R. C. Slade, *J. Chem. Soc.* (*A*), 1971, 3741.

[11] J. E. O'Connor and E. L. Amma, *Inorg. Chem.*, 1969, **8**, 2367.

and its temperature-dependence, and the magnetic anisotropy. Demonstration of the final results conveniently begins with the spectrum.

TABLE 3

Interpolated crystal and powder magnetic data for $Mn(tu)_4Cl_2$ in the temperature range 300—80 K

T/K	$10^6\bar{\chi}_M'$/c.g.s.u.	$10^6\Delta\chi_M'$/c.g.s.u.	$\bar{\mu}$/B.M.
300	14,940	34	5·99
290	15,480	36	5·99
280	16,030	38	5·99
270	16,640	41	5·99
260	17,300	44	6·00
250	18,010	47	6·00
240	18,790	51	6·01
230	19,630	56	6·01
220	20,620	61	6·02
210	21,600	67	6·02
200	22,690	74	6·03
190	23,940	81	6·03
180	25,320	89	6·04
170	26,770	99	6·03
160	28,410	112	6·03
150	30,390	126	6·04
140	32,660	142	6·05
130	35,300	163	6·06
120	38,400	190	6·07
110	42,100	227	6·09
100	46,600	275	6·11
90	52,160	339	6·13
80	59,230	418	6·16
		$\chi\perp > \chi\parallel$	

The fine structure around 6500 cm^{-1} is assigned to vibrational overtones of the ligands, being observed[10] in the spectra of $Co(tu)_4Cl_2$ and $Cd(tu)_4Cl_2$ and (partly observed) of $Ni(tu)_4Cl_2$.[9] The main band centred at *ca.* 8500 cm^{-1} would be assigned as $^5T_{2g} \longrightarrow {^5E_g}$ in O_h symmetry, putting Dq as *ca.* 850 cm^{-1}, and should be the only spin-allowed band(s). The features at 13,000 and *ca.* 16,000 cm^{-1} are then assigned as spin-forbidden transitions.

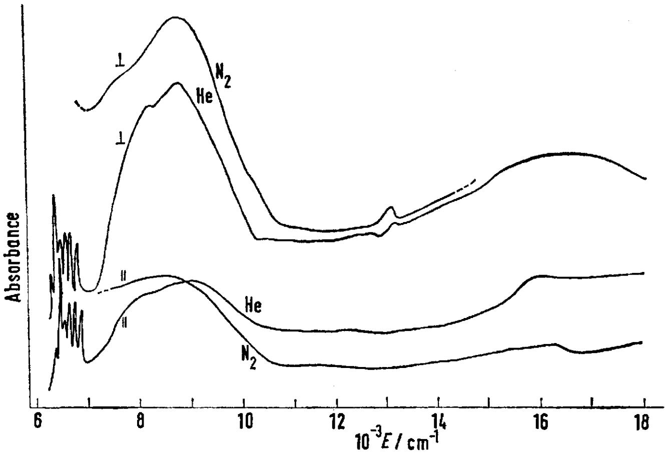

FIGURE 1 Polarized crystal spectra of $Fe(tu)_4Cl_2$ at liquid N_2 and liquid He temperatures

Some sharpening of the spectra is observed on cooling to liquid-helium temperatures, there being loss of intensity on the low-energy side of the main band, consistent with the removal of ' hot bands '. The main band is substantially perpendicularly polarized and this is the main indication of a departure from O_h symmetry. The schematic splitting of the cubic-field spin-quintet terms in D_{4h} symmetry is shown in Figure 2. Spin-orbit coupling being neglected, simple dipolar-coupling selection rules would favour a ^5E_g ground term as the transitions $^5E_g \longrightarrow {^5B_{1g}}$ and $^5E_g \longrightarrow {^5A_{1g}}$ would both be perpendicularly polarized but orbitally disallowed in parallel polarized light. A $^5B_{2g}$ ground term would tend to favour a parallel polarized spectrum. However, little weight can be placed on these polarization predictions in centrosymmetric molecules, particularly as the excited term splitting $^5B_{1g}$–$^5A_{1g}$ is too small to be certainly resolved. There is some indication of a shoulder at *ca.* 8100 cm^{-1} in the 5 K parallel polarized spectrum, possibly supported by the perpendicular polarized spectra. We suggest that a $^5B_{1g}$–$^5A_{1g}$ splitting of 1000 cm^{-1} is just possible but that such a value should be regarded as an upper limit. Band origins are likely to be somewhere between 7000 and 9000 $cm.^{-1}$ The theoretical splitting of the ^5E_g (O_h) term, spin–orbit coupling being neglected, is given by $4Ds + 5Dt$. A maximum splitting of 1000 cm^{-1} implies either that Ds and Dt are both small (say, 100 cm^{-1} each) or, if large, that they have opposed signs. We may expect Dt to be less than 200 cm^{-1} [by comparison with the spectrochemical series, and with $Co(tu)_4Cl_2$ and $Ni(tu)_4Cl_2$] being the difference between Dq(Cl) and Dq(tu) but we have no idea initially of the size of Ds. For this we must consider the magnetic properties of $Fe(tu)_4Cl_2$.

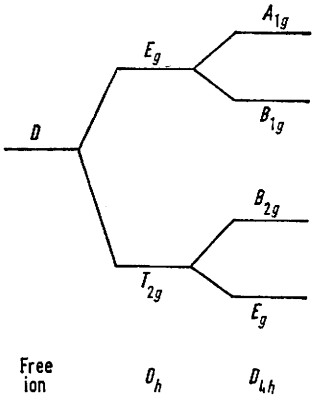

FIGURE 2 Splitting of ^5D term in D_{4h} crystal field

Figure 3 shows calculated mean moments and anisotropies at 300 and 100 K for a wide range of Ds values. The behaviour of the anisotropies resembles that in tetrahedral copper(II) ions[12] under tetragonal distortion in that positive anisotropies ($\mu_\parallel > \mu_\perp$) occur for negative and positive Ds values. Experimental values for $Fe(tu)_4Cl_2$ are indicated on the right of the diagram and show that anisotropies can be fitted with Ds positive and very small, or negative and necessarily greater than 1000 cm^{-1}. Small variations in Dt shift the curves

---

[12] M. Gerloch, *J. Chem. Soc.* (*A*), 1968, 2023.

in Figure 3 along the abscissa by a small amount with an almost insignificant change in shape. The mean moments in Figure 3 cannot fit experiment at either of these *Ds* values and as reduction in *k* and ζ will generally reduce moments, the choice of *Ds ca.* -1000 cm^{-1} is effectively removed. Figure 4 shows similar functional dependence of $\bar{\mu}$ and $\Delta\mu$ values as Figure 3 but over a much more restricted *Ds* range. Again experimental values for Fe(tu)$_4$Cl$_2$ are shown, now at 300, 100, and 5 K. Reasonable fits for $\bar{\mu}$ at these temperatures may be found for *Ds ca.* -500 cm^{-1}, but the $\Delta\mu$ values are not reproduced, even with regard to sign. For the same *Dq*(tu) value (800 cm^{-1}) but *Dq*(Cl) being varied from 800 to 900 cm^{-1} (*i.e.*, *Dt* from 0 to 57 cm^{-1}) the curves in Figure 4 retain essentially the same shape but move toward more negative *Ds* values by *ca.* 120 cm^{-1}. It is clear that reasonable variation of *Dt* values will not permit simultaneous fits to anisotropies and mean moments for the conditions of Figure 4. We therefore investigate the behaviour of moments with respect to ζ and *k*.

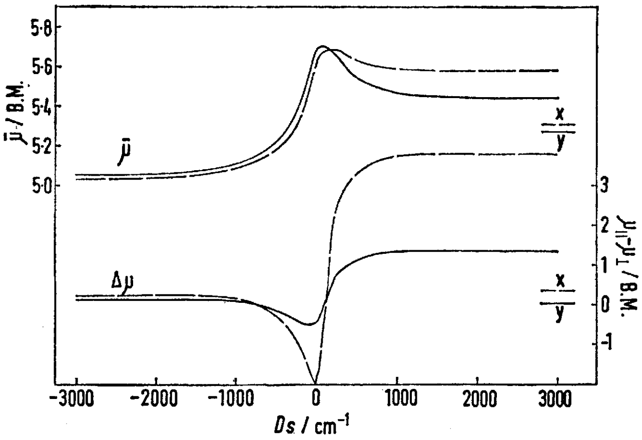

FIGURE 3 Calculated $\bar{\mu}$ and $\Delta\mu$ values for d^6 system in D_{4h} symmetry as functions of *Ds*. $Dq = 800$, $Dt = 0$, $\zeta = 400$ cm^{-1}, and $k = 1{\cdot}0$; Full lines, 300 K; broken lines, 100 K; experimental values are marked X and Y at 100 and 300 K respectively

Some typical behaviour is shown in Figure 5 where moments at 300 and 100 K are plotted as functions of *k* for a family of ζ values. Lowering of *k* reduces moments at either temperature in a linear fashion. Reduction of ζ can affect mean moments in either direction, increasing them at 100 K, reducing those at 300 K. A perusal of curves like those in Figure 4 suggests strongly that the small positive anisotropy observed for Fe(tu)$_4$Cl$_2$ must be fitted where those calculated nearly vanish, as at A–A [Figure 4(b)], and that mean moments $\bar{\mu}$ must be brought into line by reduction of *k* and ζ.

Free variation of all parameters (*Dq*, *Dt*, *Ds*, *k*, and ζ) would be computationally uneconomic and lack definition in our main point of interest, namely approximate values for, and the relation between, *Dt* and *Ds*. Accordingly, we have kept *Dq* fixed at 800 cm^{-1}. This seems reasonable in view of the main spectral band and in that $\bar{\mu}$ values are not very sensitive to small changes (say 10%) in *Dq*. Anisotropies are determined much more by *Dt* and *Ds* than by *Dq* so that a large error in *Dq* would be taken up essentially by small errors in *Dt* and *Ds*. We also fix the relation between *k* and ζ as $k = \zeta/\zeta_0$ in common with other studies.[10] As discussed later this is likely to be an inadequate approximation for all but semiquantitative estimates of the remaining parameters but might be improved in retrospect. To obtain calculated anisotropy behaviour like that at A–A in Figure 4(b) we require *Ds* values near to zero and from Figure 4(a) we note how this

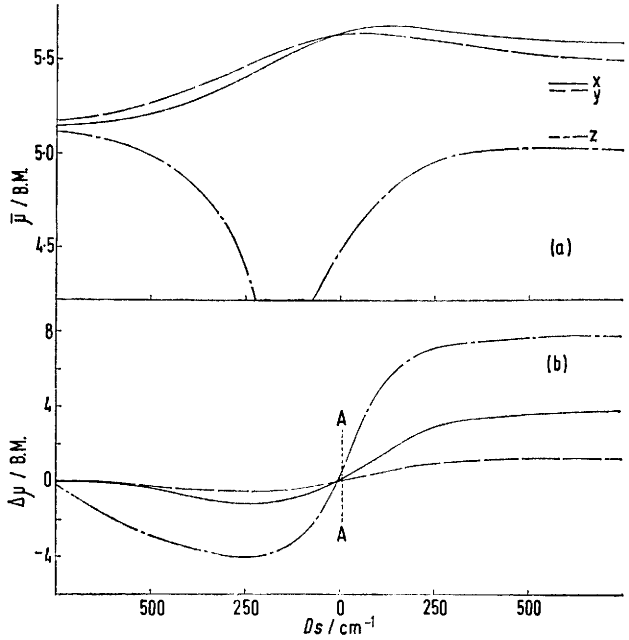

FIGURE 4 Calculated (a) $\bar{\mu}$ and (b) $\Delta\mu$ values as functions of *Ds* for expanded *Ds* scale; same conditions as for Figure 3; ---- 300 K; —— 100 K; —·—·— 5 K; experimental values are indicated X, Y, and Z

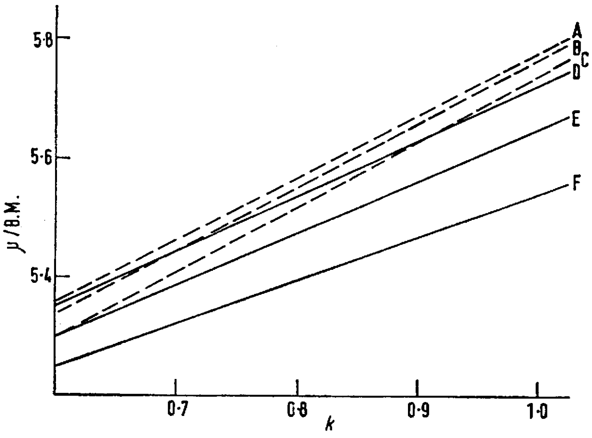

FIGURE 5 Mean moments as functions of *k* and ζ; $Dq = 800$, $Dt = 0$, $Ds = 0$ cm^{-1}; full lines, 300 K; broken lines, 100 K; curves A and F, $\zeta = 240$ cm^{-1}; curves B and E, $\zeta = 320$ cm^{-1}; curves C and D, $\zeta = 400$ cm^{-1}

corresponds to nearly equal values for $\bar{\mu}(300)$ and $\bar{\mu}(100)$ and, most important, that these are maximal and fairly insensitive to the value of Ds in that region. Figure 5 was constructed for such conditions and so suggests consideration of k values $(=\zeta/\zeta_0)$ in the region 0·6—0·8.

Accordingly, within this region of k and ζ values for $Dq = 800$ cm^{-1}, we varied Ds and Dt to obtain anisotropy values which calculate like those in the region A–A in Figure 4(a) together with absolute moments in fair agreement with experiments. The most sensitive criterion is the sign and magnitude of $\Delta\mu$. Most Ds–Dt combinations fail to reproduce the A–A condition even approximately. However, there remains still considerable ambiguity in Ds–Dt combinations which do reproduce observed $\Delta\mu$ values. It is encouraging to observe how only these conditions also permit fits to $\bar{\mu}$(5 K), the values of $\bar{\mu}$(300 K) and $\bar{\mu}$(100 K) being sensitive to k and ζ rather than Ds and Dt. Figure 6 illustrates the sort of fitting procedure involved. We observe how the calculated $\bar{\mu}$(5 K) values maximize near these co-ordinates, so confirming the results from the anisotropies nicely. The fits are not accurate. In particular, the temperature-dependence of $\bar{\mu}$ in the range 300—100 K is calculated the wrong way round. The change of $\bar{\mu}$ in this range is experimentally small, however, and the calculated trend might be reversed by relaxing the condition $k = \zeta/\zeta_0$ as noted in connection with Figure 5 but we are content with the semiquantitative results so far obtained. Investigation of many more graphs like those in Figure 6 leads to the general conclusion that $0{\cdot}6 < k < 0{\cdot}7$ with the lower value being favoured. A slightly smaller ratio such that $k < \zeta/\zeta_0$ might improve the fits. The relation between Ds and Dt implied by graphs like those in Figure 6 is roughly independent of k in this region and is summarized by the linear relationship shown in Figure 7.

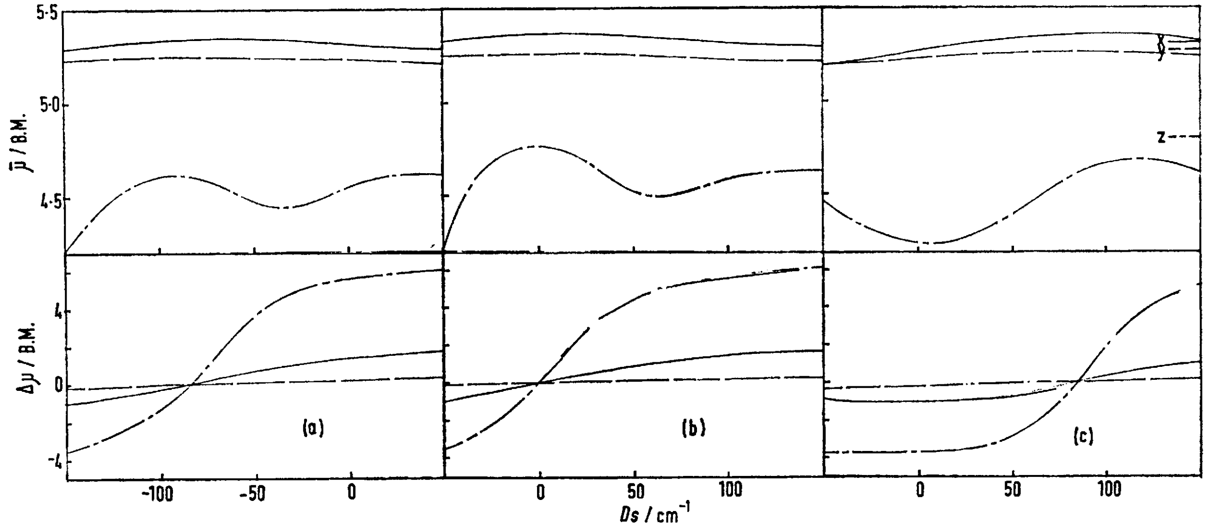

FIGURE 6 Fitting experimental anisotropies and mean moments of Fe(tu)$_4$Cl$_2$; $B = 790$, $C = 3160$, $\zeta = 240$, $Dq = 800$ cm^{-1}, $k = 0{\cdot}6$; see text; — — 300 K; —— 100 K; — · — · — 5 K; (a) $Dt = -50$ cm^{-1}; (b) $Dt = 0$; (c) $Dt = +50$ cm^{-1}; experimental values are indicated X, Y, and Z

Thus the magnetism of Fe(tu)$_4$Cl$_2$, particularly the sign and order of magnitude of anisotropy, fixes a relationship of the quadrate crystal-field parameters such that Ds and Dt have the same sign with the magnitude of Ds being about 1·8 times that of Dt. The small spectral splitting $^5A_{1g}$–$^5B_{1g}$ noted earlier implied that if Ds and Dt had the same sign then they must both be small as $4Ds + 5Dt <$ *ca.* 1000 cm^{-1}. Using the rough relation from Figure 7, we have, therefore, $|Dt| <$ *ca.* 85 cm^{-1} with Ds *ca.* 1·8 Dt.

Dichlorotetrakis(thiourea)manganese(II).—Magnetic and spectral properties of complexes of the half-filled d shell in manganese(II) are very similar to those for iron(III)· Magnetic anisotropy in high-spin d^5 systems arises from small zero-field-splittings (z.f.s.) of the ^6S ground term. Extremely small z.f.s. in a perfectly octahedral d^5 system is considered to arise from spin–spin coupling

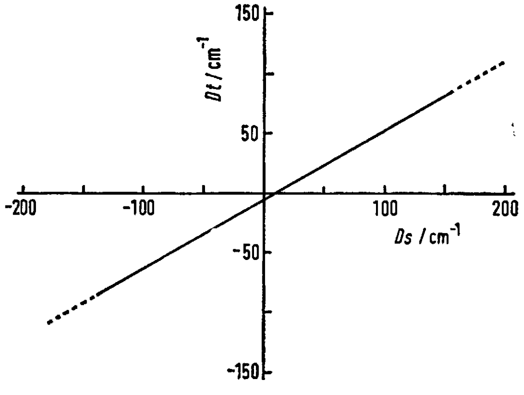

FIGURE 7 Relationship between Ds and Dt values derived from fitting procedure in Figure 6, when $k = \zeta/\zeta_0 = 0{\cdot}6$—0·7

effects,[13,14] but in systems of lower symmetry, as here, the combined effects of spin–orbit coupling and the low-symmetry field completely dominate such spin–spin coupling effects. Griffith[15] has pointed out that free-ion spin–orbit coupling selection rules define the only direct spin–orbit interaction with the ground ^6S term as being with the excited ^4P term. In any symmetry lower than cubic, spin–orbit coupling with the ligand-field-split components of the ^4P term removes all but the Kramers degeneracy of the ground term as in Figure 8. For tetragonal geometries (or axial geometries in general) the z.f.s. is expressed in terms of the parameter D as shown in Figure 8.

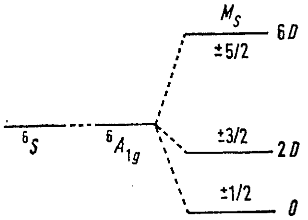

FIGURE 8 Zero-field-splitting of ^6S term in d^5 system

Griffith[16] has given a simple relationship (1) expressing the z.f.s. parameter D in terms of the spin–orbit coupling coefficient ζ and the low-symmetry splitting of the ^4P term, where $E_\parallel$ and $E_\perp$ refer to the energies

$$D = \frac{\zeta^2}{5}\left[\frac{1}{E_\parallel} - \frac{1}{E_\perp}\right] \qquad (1)$$

of the $^4A_2$ and ^4E components of ^4P. Our present interest, however, is in estimating signs and magnitudes for the crystal-field parameters Dt and Ds. This requires a knowledge of the dependence of $E_\parallel$ and $E_\perp$ on these parameters. We have calculated this dependence for a limited number of parameter values using the usual tensor operators for crystal-field and spin–orbit coupling and a free-ion term function basis. Performing the calculations in this way immediately, and powerfully, reveals both new and well known pecularities of the half-filled-shell configuration.

First, all diagonal-reduced matrix elements of any crystal-field potential or of spin–orbit coupling vanish identically because the d^5 configuration is its own hole equivalent. Hence all splittings and energy shifts in Tanabe–Sugano or similar diagrams for d^5 result solely from off-diagonal matrix elements between free-ion terms. In particular, this means that a calculation of the splitting of the ^4P term in the present D_{4h} symmetry will fail if the basis functions are restricted to those of ^4P. Thus, although spin–orbit selection rules dictate that only components of ^4P connect with the ^6S ground term, any calculation of the z.f.s. effect must include other spin-quartet states also. The free-ion ^4G and ^4P terms are of similar energy with ^4F lying much higher. We have therefore performed calculations within the restricted basis (^4G, ^4P, ^6S) which should be sufficient for a semiquantitative correlation of z.f.s. and ligand-field parameters.

The second important point, which follows from the symmetry of rotation operators, is that the second-order term in the ligand-field potential, $Y_2{}^0$, is inoperative within the spin-quartet levels. This can be seen from the vector triangle rule. The only off-diagonal crystal-field-reduced matrix elements occurring for ^4P and ^4G terms on D_{4h} symmetry are $\langle {}^4P \| U2 \| {}^4G \rangle$ and $\langle {}^4P \| U4 \| {}^4G \rangle$. The second of these is non-zero (actually $\sqrt{2}$), while the orbital quantum numbers 1, 2, and 4 in the second-order term cannot form a vector triangle. Therefore, within the present ^6S–^4P–^4G basis set, crystal-field splitting of the ^4P term arises by interaction with the ^4G term under the action of fourth-order harmonics alone. In this way Ds is an irrelevant parameter here. (The same vector triangle rule determines the spin–orbit selection rule in that, within the present basis, the only non-zero reduced matrix element of a tensor operator of rank one is $\langle {}^6S \| U1 \| 4P \rangle$, the quantum numbers 0, 1, and 1 forming a triangle.) In summary, the schematic matrix of ^6S, ^4P, and ^4G under the combined perturbation of a D_{4h} crystal-field and spin-orbit coupling is represented as in Figure 9. The parameter-dependence of matrix elements is depicted rather than their actual values.

$$\begin{array}{c|cc|c|}
 & {}^4G & {}^4P & {}^6S \\
\hline
{}^4G & 0 & Dq\ ,\ Dt & 0 \\
\hline
{}^4P & Dq\ ,\ Dt & 0 & \zeta \\
\hline
{}^6S & 0 & \zeta & 0 \\
\hline
\end{array}$$

FIGURE 9

Calculations have been performed by use of the free-ion interelectron repulsion parameters for Mn^{II}: B 960 cm^{-1}, $C = 4B$. Representative values of Dq 1000 cm^{-1} and 300 cm^{-1} were also assumed. Values for Dt were allowed to range between ± 200 cm^{-1}. In Figure 10 we show behaviour of the quartet energy levels as functions of Dt. Only components of the $^4T_{1g}$ (O_h) terms are included as no other splittings take place within the ^4G term without inclusion of the ^4F term. The main feature to emerge is that the relative ordering of the $^4A_2$ and ^4E levels is determined solely by the sign of Dt. It is the admixture of the lower two quartet levels into the ground ^6S term which essentially determines the z.f.s., for although these levels formally derive

---

[13] H. Watanabe, *Progr. Theor. Phys.*, 1957, **18**, 405.

[14] M. J. D. Powell, J. R. Gabriel, and D. F. Johnston, *Phys. Rev. Letters*, 1960, **5**, 145.

[15] J. S. Griffith, 'Quantum Aspects of Polypeptides and Polynucleotides,' Biopolymer Symposium 1, Interscience, New York, 1964.

[16] J. S. Griffith, *Mol. Phys.*, 1904, 213.

from ${}^4G$ rather than ${}^4P$, the proximity of these two free-ion terms establishes considerable mixing of P and G characters. The sign of zero-field-splitting is thus determined by the sign of Dt and as the sign of anisotropy is fixed[17] by the sign of D we have a general rule for high-spin d^5 complexes, *e.g.*, $\mathrm{Fe^{III}}$ or $\mathrm{Mn^{II}}$ in D_{4h} symmetry, *viz.*, $\mu_\perp > \mu_\parallel$ implies $D > 0$ implies Dq (equatorial) $> Dq$ (axial) and *vice versa*.

A determination of the magnitude of Dt from $\Delta\mu$, however, requires knowledge of the magnitude of Dq and ζ. While estimates of these parameter values can be made, the greatest problem rests with the experimental accuracy of our measurement of magnetic anisotropy. The correction for the diamagnetic anisotropy of the cadmium analogue is very small but, in measuring anisotropies of *ca.* 100×10^{-6} c.g.s.u. in a crystal with a mean susceptibility of *ca.* $20{,}000 \times 10^{-6}$ c.g.s.u., corrections for crystal-shape anisotropy effects are likely to be significant. While confident of the *sign* of $\Delta\mu$ we prefer not to rely upon the magnitude of $\Delta\mu$. Accordingly we report for $\mathrm{Mn(tu)_4Cl_2}$ that $\mu_\perp > \mu_\parallel$ giving Dt positive, *i.e.* Dq(thiourea) $> Dq$(chlorine).

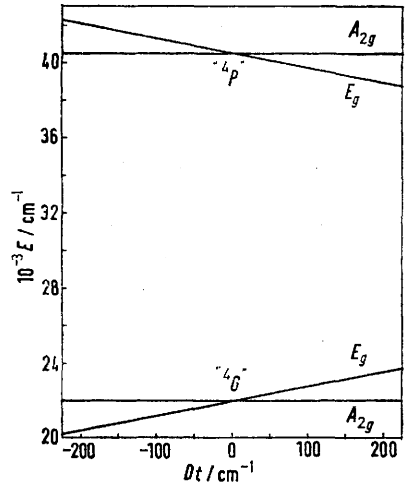

FIGURE 10 Splitting of ${}^4T_{1g}$ (O_h) terms as functions of Dt; $B = 960$, $C = 3840$, $Dq = 1000$, $\zeta = 300$ cm^{-1}. Free-ion parentage is indicated but considerable ' scrambling ' has occurred

Conclusions.—The molecular structure[18] of the nickel(II) analogue, $\mathrm{Ni(tu)_4Cl_2}$, is non-centrosymmetric and involves anomalously long Ni–Cl bonds. The sign of Dt was unambiguously determined[9] in that system from the sign of the magnetic anisotropy but unlike the case of $\mathrm{Mn(tu)_4Cl_2}$, Ds was a significant feature of the analysis. The molecular structure[11] of the cobalt(II), iron(II), and manganese(II) complexes are all centrosymmetric with more ' normal ' metal–halogen bond lengths. In these three molecules, Dt is a much smaller quantity than in the nickel compound (or so we assume for the $\mathrm{Mn^{II}}$ case) and in the cases of the cobalt(II)[10] and iron(II) systems the sign of Dt could not be established. In both cases, Ds appears to have a small value, being *ca.* twice the size of Dt and of the same sign. Comparison with $\mathrm{Ni(tu)_4Cl_2}$ and the positions of thiourea and chlorine in the spectrochemical series both tend to favour positive values of Dt in this series and it is encouraging to find this confirmed in the one other case where an ambiguity does not exist, namely $\mathrm{Mn(tu)_4Cl_2}$.

Overall, we may conclude that chlorine occupies a very slightly lower place in the spectrochemical series than thiourea and that this difference is exaggerated by steric and hydrogen-bonding factors in the nickel(II) compound. It appears that Ds values are small: a ratio $Ds : Dt$ of *ca.* 2 would be roughly compatible with the experimental data of all four molecules.

The analyses of the results from the molecules from spectral and magnetic single-crystal data all illustrate important general features of the model. For nickel(II) and manganese(II), the sign of Dt is most likely to be determined by the sign of the magnetic anisotropy. Iron(II) and cobalt(II) systems in this symmetry, however, present a number of difficulties and ambiguities which make fitting theory to experiment a long and ambiguous process. This is particularly so for nearly isotropic systems like these where Dt is so small. The models we have described should be simpler to use and less ambiguous for more strongly distorted systems.

APPENDIX

Defining effective equatorial bond lengths as a and axial ones as b we use the standard definitions (2)—(5), where G_n is given by the integral (6). In D_{4h} symmetry

$$Cp(a) = \tfrac{2}{7}ze^2G_2(a) \tag{2}$$

$$Dq(a) = \tfrac{1}{6}ze^2G_4(a) \tag{3}$$

$$Cp(b) = \tfrac{2}{7}ze^2G_2(b) \tag{4}$$

$$Dq(b) = \tfrac{1}{6}ze^2G_4(b) \tag{5}$$

$$G_n = \int_0^\infty R^2(3d)r^2 \cdot \frac{r_<^{\,n}}{r_>^{\,n+1}} \cdot \mathrm{d}r \tag{6}$$

we use equations (7)—(9).

$$Dt = \tfrac{4}{7}[Dq(a) - Dq(b)] \tag{7}$$

$$Ds = Cp(a) - Cp(b) \tag{8}$$

$$\kappa = Ds/Dt \tag{9}$$

All calculations were performed in J, M_J quantization by use of the programme discussed in ref. 19.

We thank Dr. D. J. Mackey for use of his computer programme and the S.R.C. for research grants (to W. R. S.).

[2/046 *Received*, 10*th January*, 1972]

---

[17] M. Gerloch, J. Lewis, and R. C. Slade, *J. Chem. Soc.* (*A*), 1969, 1422.

[18] A. Lopez-Castro and M. R. Truter, *J. Chem. Soc.*, 1963, 1309.

[19] M. Gerloch and D. J. Mackey, *J. Chem. Soc.* (*A*), 1971, 2605.